HHS Public Access

Author manuscript

ACS Nano. Author manuscript; available in PMC 2020 August 20.

Published in final edited form as:

ACS Nano. 2020 July 28; 14(7): 8103–8115. doi:10.1021/acsnano.0c00999.

Phospholipase A_2 Inhibitor-Loaded Phospholipid Micelles Abolish Neuropathic Pain

Sonia Kartha, **Lesan Yan**, **Meagan E. Ita**, **Ahmad Amirshaghaghi**, **Lijun Luo**, **Yulong Wei**, **Andrew Tsourkas**

Department of Bioengineering, University of Pennsylvania, Philadelphia, Pennsylvania 19104, United States;

Beth A. Winkelstein

Department of Bioengineering, University of Pennsylvania, Philadelphia, Pennsylvania 19104, United States;

Department of Neurosurgery, University of Pennsylvania, Hospital of the University of Pennsylvania, Philadelphia, Pennsylvania 19104, United States;

Zhiliang Cheng

Department of Bioengineering, University of Pennsylvania, Philadelphia, Pennsylvania 19104, United States;

Abstract

Treating persistent neuropathic pain remains a major clinical challenge. Current conventional treatment approaches carry a substantial risk of toxicity and provide only transient pain relief. In this work, we show that the activity and expression of the inflammatory mediator secretory phospholipase-A_2 ($sPLA_2$) enzyme increases in the spinal cord after painful nerve root compression. We then develop phospholipid micelle-based nanoparticles that release their payload in response to $sPLA_2$ activity. Using a rodent model of neuropathic pain, phospholipid micelles loaded with the $sPLA_2$ inhibitor, thioetheramide-PC (TEA-PC), are administered either locally or intravenously at the time of painful injury or 1–2 days afterward. Local micelle administration immediately after compression prevents pain for up to 7 days. Delayed intravenous administration of the micelles attenuates existing pain. These findings suggest that $sPLA_2$ inhibitor-loaded micelles can be a promising anti-inflammatory nanotherapeutic for neuropathic pain treatment.

GRAPHICAl ABSTRACT:

Corresponding Author: Zhiliang Cheng – Department of Bioengineering, University of Pennsylvania, Philadelphia, Pennsylvania 19104, United States; zcheng@seas.upenn.edu.

Author Contributions

S.K. and Z.C. conceived and performed all designs, experiments, and characterization in this study, as well as prepared the manuscript and figures. L.Y. and A.A. prepared and characterized the nanoparticles. M.I. performed *in vitro* cytotoxicity experiments. L.L. collected blood and determined the circulation time of the nanoparticles. W.Y. performed the organ toxicity study. A.T., B.W., and Z.C. conceived and oversaw all aspects of this study and prepared the manuscript.

Supporting Information

The Supporting Information is available free of charge at https://pubs.acs.org/doi/10.1021/acsnano.0c00999.

Additional information (PDF)

The authors declare no competing financial interest.

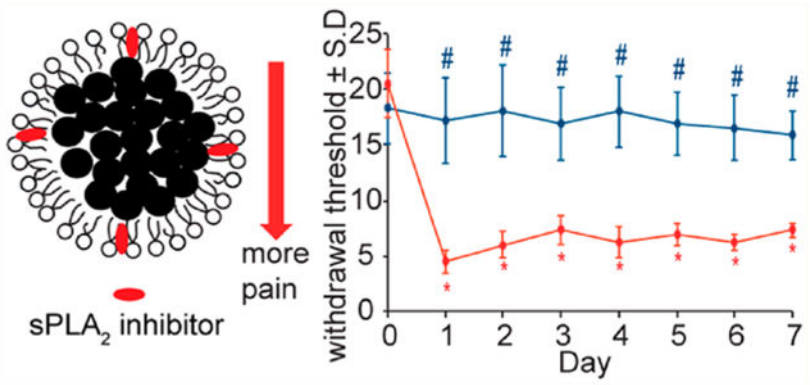

Keywords

phospholipase; inhibitor; phospholipid micelles; inflammation; neuropathic pain

Neuropathic pain, which develops from direct or secondary neural tissue injury or damage, occurs in approximately 10% of the U.S. population[1] and often persists for several years or even a lifetime after an initial injury.[2] Despite its prevalence, neuropathic pain remains largely resistant to treatment,[3,4] leading to chronic disability,[5] with staggering societal and economic costs.[6,7] Current neuropathic pain treatments include surgical intervention and pharmacologic approaches, but are largely ineffective, providing only transient pain relief.[7–10] Although treatment of neuropathic pain through opioid[11] and nonopioid analgesics[12] has been extensively pursued, these approaches are often accompanied by undesired side effects including addiction and increased pharmacological tolerance.[13] Accordingly, there is a tremendous need to develop new interventional platforms for greater effectiveness to treat chronic neuropathic pain.

In addition to the primary injury to neural tissue that occurs with nerve root trauma and spinal cord injury,[14] painful neuropathic injuries are accompanied by a robust secondary neuroinflammatory response, both at the site of injury and remote to it in the spinal cord.[15–17] Many different animal models of neuropathic pain have defined a host of inflammatory cascades both at the site of injury and in the central nervous system (CNS),[18–23] contributing to central sensitization that is responsible for persistent pain.[24–27] During central sensitization there is increased neuronal hyperexcitability and spontaneous activity in spinal neurons, which can result from and be exacerbated by inflammatory mediators that directly act on neurons.[28] Among the potent inflammatory mediators involved in spinal neuroimmune regulation of pain is the family of phospholipase-A_2 (PLA_2) enzymes. These enzymes recognize and catalytically hydrolyze the sn-2 ester bond of glycerophospholipids, releasing free fatty acids, such as arachidonic acid (AA) and lysophospholipids, that are involved in tissue damage and neuronal injury, as well as a host of inflammatory and neurological disorders.[29,30] Many studies have reported expression of the secretory PLA_2 ($sPLA_2$), an isoform of the PLA_2 enzyme, to be associated with a number of painful pathologies characterized by inflammation, such as disc herniation, disc degeneration, discogenic pain, and neuropathic pain.[31–36] $sPLA_2$ is normally present in the mammalian

spinal cord and brain.[37,38] Yet, under pathological conditions $sPLA_2$ can be induced by multiple cascades and effector molecules including inflammatory cytokines,[39] free radicals,[40] and excitatory amino acids.[41] Elevated $sPLA_2$ expression after neuropathic injury is observed both centrally in the spinal cord and in the peripheral dorsal root ganglion (DRG), both anatomic sites that contribute to the potentiation and amplification of chronic pain after trauma.[42,43] As such, if $sPLA_2$ is a sensitive marker for spinal neuroinflammation and painful neuropathic injury, it can be exploited to also act as a therapeutic target for pain treatment. However, no study has harnessed the specific $sPLA_2$ response for the treatment of neuropathic pain.

Clinical management of neuropathic pain is further complicated by lack of effective drug delivery. Systemic delivery of small-molecule drugs provides only a small portion of medication at the site of injury, and even less drug is delivered to the spinal cord, where pain modulation occurs.[8,12] Yet, delivery of drugs directly to the spinal cord *via* intrathecal injection is invasive, imposes toxicity to uninjured spinal levels, and is difficult to perform in nonhospital settings.[10,44,45] Recently, nanoparticle-based drug delivery has been extensively explored in the treatment of cancer.[46] Such drug delivery systems not only increase the concentration of drug that can be delivered to target tissues, lowering the overall dose needed, but also reduce off-target toxicity and side-effects.[10,45] Imaging agents can also be incorporated into these systems as theranostic agents,[47] which may be promising for painful neuropathy treatment, which is often hindered by heterogeneous diagnostic criteria.[48] A delivery platform that enables tunable drug release based on the pathological conditions that are induced by the pain state itself offers a long-term clinical option to treat patients with neuropathic pain. Therefore, in this study we first defined if spinal $sPLA_2$ expression after a nerve root compression injury is specific to a painful state, enabling its possible utility as a potential therapeutic target for pain modulation. On the basis of those positive findings, we fabricated $sPLA_2$ inhibitor-loaded micelle nanoparticles (Figure 1A). The effectiveness of these $sPLA_2$ inhibitor-loaded micelles was tested in both preventing and abolishing pain and spinal inflammation using both local and systemic administration paradigms in a well-established rodent model of persistent neuropathic pain (Figure 1B).

RESULTS AND DISCUSSION

Spinal $sPLA_2$ Expression after Painful Neuropathic Injury to the Nerve Root.

Spinal $sPLA_2$ is elevated only after a painful nerve root injury. In fact, early (at day 1) after nerve root compression (Figure 2A), spinal $sPLA_2$ increases in the spinal cord only after a painful compression, with the extent of spinal $sPLA_2$ 1.85 ± 1.20-fold greater than levels at that time after nonpainful root compression ($p = 0.048$) and 1.97 ± 0.82 times the levels after a nonpainful sham surgery ($p = 0.044$) (Figure 2B). Further, at day 7, the increase in spinal $sPLA_2$ expression is even more robust, with further increases ($p = 0.043$) by 48.7 ± 9.4% over levels at day 1 (Figure 2). Although $sPLA_2$ levels in both the nonpainful and sham control groups increase at day 7 from levels at day 1, those increases are not significant (Figure 2B). At day 1, the majority of spinal $sPLA_2$ is expressed in microglia, with the lowest extent of $sPLA_2$ expression observed in astrocytes (Figure 2C). Similar to total spinal $sPLA_2$ levels, both microglial and neuronal $sPLA_2$ expression at day 1 are significantly

higher ($p < 0.006$ and $p < 0.038$, respectively) after painful injury compared to nonpainful and sham surgeries (Figure 2D). There are no differences among groups observed for astrocytic $sPLA_2$ levels at day 1. Together, these data support that increased spinal $sPLA_2$ expression appears to be sensitive to a painful injury and may be an appropriate molecular target for neuropathic pain treatment.

Synthesis and Characterization of $sPLA_2$ Inhibitor-Loaded Phospholipid Micelles.

Based on the findings that spinal $sPLA_2$ expression increases after painful neuropathic injury to the nerve root, therapeutic nanoparticles were prepared by incorporating $sPLA_2$ inhibitor thioetheramide-PC (TEA-PC) into small hydrophobic superparamagnetic iron oxide nanoparticle (SPION, 7 nm, Figure S1)-loaded phospholipid micelles. Due to the *amphiphilic nature* of phospholipid molecules, these SPIO-loaded micelles were highly soluble in aqueous solutions. Dynamic light scattering (DLS) revealed that the $sPLA_2$ inhibitor-loaded phospholipid micelles had a mean diameter of 60 nm with a polydispersity index (PDI) of 0.20 in water (Figure 3A). However, a large aggregation for the micelles was found when the amount of incorporated $sPLA_2$ inhibitor increased from 1 mg to 2 mg in the preparation of the current formulation. Given the drug-loading efficiency and appropriate size, we therefore chose to prepare a micelle formulation with 1 mg $sPLA_2$ inhibitor loading for further *in vitro* and *in vivo* testing. The morphologies of these micelles were further confirmed by transmission electron microscopy (TEM) (Figure 3B), in which the SPIONs were found to be tightly packed into a spherical core. The SPIO-loaded micelles exhibited superparamagnetic properties with an R_2 value of 464 mM^{-1} s^{-1} (Figure S2). Micelle stability was also evaluated by incubating $sPLA_2$ inhibitor-loaded micelles in PBS buffer for up to 7 days. No changes were observed in the hydrodynamic diameter of the micelles at days 1 or 7, suggesting there was no aggregation or precipitation of micelles during the incubation period (Figure S3).

To study the ability of $sPLA_2$ inhibitor-loaded micelles to inhibit $sPLA_2$ enzyme, phospholipid hydrogenated soy phosphatidylcholine (HSPC) liposomes doped with the fluorescent lipid 1-palmitoyl-2-{6-[(7-nitro-2–1,3-benzoxadia-zol-4-yl)amino]hexanoyl}-*sn*-glycero-3-phosphocholine (NBD-PC) were prepared as a fluorescent sensor for $sPLA_2$ activity. The fluorophore NBD was attached to the sn-2 position of the phospholipid with a spacer (C6) between NBD and the lipid backbone since native $sPLA_2$ enzymes specifically recognize and catalytically hydrolyze the sn-2 acyl bond of phospholipids.[49] When 20 mol % NBD-PC was incorporated into the HSPC liposomal membrane, the NBD was highly quenched within the phospholipid membrane.[49] Little to no change in fluorescence was observed over a 24 h time period when these NBD-incorporated liposomes were incubated in buffer (10 mM HEPES, pH 7.4). However, a significant increase in the fluorescence intensity was observed immediately upon the addition of the preincubation mixture of control unloaded micelles (*i.e.*, no $sPLA_2$ inhibitor) and $sPLA_2$ enzyme (Figure 3C). The $sPLA_2$-induced change in fluorescence was due to the release of NBD into the surrounding bulk solution upon the hydrolysis of the phospholipid liposomal membrane by the $sPLA_2$ enzyme. The released NBD led to fluorescence dequenching, resulting in a higher fluorescence intensity. For comparison, $sPLA_2$ inhibitor-loaded micelles were also tested under similar conditions. No change in fluorescence intensity was observed when the

preincubation mixture of $sPLA_2$ inhibitor-loaded micelles and $sPLA_2$ enzyme was added into the NBD-incorporated liposomal suspension, revealing that the release of NBD was significantly inhibited. Furthermore, to evaluate if $sPLA_2$ inhibitor-loaded micelles reduced $sPLA_2$ activity in a dose-dependent manner, inhibitor micelles of three separate concentrations of $sPLA_2$ inhibitor (0–4.83 μg/mL) were incubated under a constant amount of $sPLA_2$ enzyme. Indeed, the greater reductions in the extent of fluorescence activation were observed with increasing inhibitor concentrations (Figure S4), suggesting that $sPLA_2$ inhibitor-loaded micelles inhibit $sPLA_2$ activity in a concentration-dependent manner.

To assess cytotoxicity of the $sPLA_2$ inhibitor-loaded micelles prior to *in vivo* administration, micelles were incubated for 24 h with dorsal root ganglia neurons. Incubation of the $sPLA_2$ inhibitor-loaded micelles did not reduce neuronal viability at any concentration tested compared to untreated control cultures (Figure 3D). Additionally, incubation of the $sPLA_2$ inhibitor-loaded micelles in neuronal cultures did not significantly increase cell lysis compared to control cultures, with the greatest concentration of micelles inducing 4.42 ± 1.77% lysis for the total culture (Figure S5). These data suggest that the $sPLA_2$ inhibitor-loaded micelles are safe for *in vivo* administration.

Therapeutic Efficacy Following Local Administration of $sPLA_2$ Inhibitor-Loaded Micelles.

Local administration of $sPLA_2$ inhibitor-loaded micelles immediately after a painful root compression prevents the onset of pain as early as 1 day after injury, lasting for up to 7 days (Figure 4A). Withdrawal thresholds in the ipsilateral forepaw after treatment with $sPLA_2$ inhibitor-loaded micelles are significantly higher ($p < 0.016$) than those thresholds after injury treated with unloaded micelles on all days of testing. Treatment with the control unloaded micelles does not prevent pain development, with ipsilateral paw withdrawal thresholds on all days (days 1–7) remaining significantly lower ($p < 0.0001$) than the preinjury response. Additionally, there are no significant differences between thresholds in the contralateral paws for both groups for any post-treatment day (Figure 4B).

Prussian Blue staining was performed to identify if iron oxide particles are present in the injured C7 dorsal nerve roots, after treatment with both $sPLA_2$ inhibitor-loaded micelles and control unloaded micelles. Following local administration of the $sPLA_2$ inhibitor-loaded micelles and unloaded control micelles, iron oxide particles are evident only in the injured (compressed) nerve root (Figure 4C and Figure S6), confirming accumulation of micellar treatment at the injury site. There are no iron oxide particles evident in any contralateral uninjured nerve root after either micelle treatment.

Local administration of $sPLA_2$ inhibitor-loaded micelles immediately after injury not only prevents pain but also prevents the increase in spinal $sPLA_2$ that is observed after a painful nerve root injury (Figure 4D). Spinal $sPLA_2$ expression at day 7 is significantly lower ($*p < 0.0001$) after treatment compared to $sPLA_2$ levels in the spinal cord of an untreated injury condition (Figure 4D). In addition, microglial activation, a common hallmark of spinal inflammation, was evaluated using labeling for Iba1 and is lowered in the superficial dorsal horn at day 7 after treatment with $sPLA_2$ inhibitor-loaded micelles (Figure 4E). Similar to spinal $sPLA_2$ expression, Iba1 levels are significantly reduced ($p = 0.0002$) following

treatment with $sPLA_2$ inhibitor-loaded micelles, while Iba1 levels in the untreated spinal cord remain 2.32 ± 1.25-fold over normal levels (Figure 4E).

Nanoparticle Structural Integrity during Intravenous Administration.

The $sPLA_2$ activity in the blood and C7 spinal cord tissue was measured to assess the relative levels of $sPLA_2$. $sPLA_2$ activity in ipsilateral injured spinal tissue was significantly higher, 6.07 ± 1.16-fold ($p = 0.0004$), over circulating $sPLA_2$ activity in serum samples (Figure S7A). To assess nanoparticle integrity in the presence of circulating $sPLA_2$ enzymes, fluorescence-quenched HSPC liposomes were incubated with serum that was collected 1 day after a painful injury. No significant change in fluorescence was observed, either immediately upon mixing or 24 h later (Figure S7B). Increased fluorescence, a proxy for disrupted liposomes, was observed only following the addition of Triton-X, indicating that activity from circulating $sPLA_2$ enzymes does not affect the $sPLA_2$ inhibitor-loaded phospholipid micelles.

Therapeutic Efficacy Following Delayed Intravenous Administration of $sPLA_2$ Inhibitor-Loaded Micelles.

Since local administration of $sPLA_2$ inhibitor-loaded micelles prevents the onset of pain after nerve root compression (Figure 4A) and seems to modulate spinal inflammation even at later times (Figure 4E), we sought to test if giving these $sPLA_2$ inhibitor-loaded micelles *via* systemic routes after pain has been established would be effective as a treatment to abolish or reduce pain. A pilot study was first performed by administering $sPLA_2$ inhibitor-loaded micelles on day 1 after painful nerve root injury, at the same dose shown to reduce pain when administered locally to the nerve root after compression. Following treatment only on day 1, withdrawal thresholds were significantly lower ($p < 0.0007$) on days 3–7 compared to preinjury (day 0) thresholds (Figure S8), suggesting that a single dose of micelles is not sufficient to relieve existing pain. As such, the $sPLA_2$ inhibitor-loaded micelles were given repeatedly *via* the tail vein on days 1 and 2 postinjury, at the same dose that prevents pain *via* the local administration after nerve root compression. As expected, the two groups, which received $sPLA_2$ inhibitor-loaded and unloaded micelles, subjected to painful nerve root compression exhibited a significant reduction ($p < 0.0053$) in withdrawal thresholds compared with preinjury thresholds as early as day 1 postinjury (Figure 5A). Since those behavioral assessments are made prior to any micelle treatment, withdrawal thresholds in the unloaded and inhibitor-loaded micelle groups are also significantly lower ($p < 0.001$) compared to the sham surgical control group on day 1.

However, after behavioral testing on day 1, treatment with $sPLA_2$ inhibitor-loaded micelles was given and the withdrawal threshold increases on day 2 to sham and preinjury levels, indicating less pain (Figure 5A). After the second micellar treatment dose on day 2, withdrawal thresholds are still elevated on day 3 and remain the same as preinjury through day 7 (Figure 5A). After $sPLA_2$ inhibitor-loaded micelle treatment, the responses are significantly increased ($^*p < 0.0024$) through day 7 over thresholds in the group receiving a painful nerve root compression and unloaded micelles (Figure 5A). In fact, there are no differences between the micelle treatment group and sham group on any post-treatment days. However, repeated intravenous administration of control micelles without the inhibitor

does not alter the pain response, and thresholds remain significantly lower than baseline ($p < 0.0001$) and sham surgical control responses ($p < 0.002$) (Figure 5A). Similar to local administration of $sPLA_2$ inhibitor-loaded micelles (Figure 4B), the contralateral withdrawal thresholds are not different between the two treatment groups or sham group at any day postinjury (Figure 5B). In addition, as with the local administration of $sPLA_2$ inhibitor-loaded micelles (Figure 4C), iron oxide particles localize only to the injured C7 dorsal nerve root after intravenous delivery of the $sPLA_2$ inhibitor-loaded micelles (Figure S9A), with no evidence of accumulation in the treated sham and naïve C7 nerve roots. Iron oxide particles are also observed in the white and gray matter of the ipsilateral but not the contralateral C7 spinal sections after painful injury, but not in naïve spinal tissues (Figure S9B). These studies validate sufficient selective accumulation of $sPLA_2$ inhibitor-loaded micelles to the injury C7 spinal level with systemic delivery.

Systemic treatment with $sPLA_2$ inhibitor-loaded micelles also significantly reduces ($p = 0.038$) $sPLA_2$ expression in the spinal dorsal horn compared to treatment with control unloaded micelles at day 7, almost to levels of a normal naïve spinal cord (Figure 5C). Similarly, $sPLA_2$ expression in the DRG is also significantly ($p = 0.002$) reduced by 2.29 ± 0.39-fold to normal levels, after treatment with $sPLA_2$ inhibitor-loaded micelles (Figure 5D). Similar to local administration, systemic treatment with $sPLA_2$ inhibitor-loaded micelles also significantly reduces ($p < 0.0002$) spinal Iba1 expression to normal levels compared to treatment with unloaded micelles alone (Figure S10A). Systemic treatment with inhibitor micelles also significantly decreased ($p = 0.0002$) microglial $sPLA_2$ expression, to normal levels, compared to treatment with unloaded micelles (Figure S10B and C). At day 7, spinal Iba1 expression after treatment with unloaded micelles is significantly higher ($p < 0.0002$) than treatment with $sPLA_2$ inhibitor-loaded micelles and normal (uninjured) levels. Consistent with the histological evidence of micelle accumulation at the site of injury (nerve root) and spinal cord (Figure S9), decreased $sPLA_2$ expression in the spinal cord and DRG after systemic micellar treatment further suggests that the $sPLA_2$ inhibition occurs at the injured C7 spinal level.

Pharmacokinetics, *In Vivo* Toxicity, and Micelle Accumulation Following Delayed Intravenous Administration of $sPLA_2$ Inhibitor-Loaded Micelles.

Following intravenous injection of rhodamine-labeled $sPLA_2$ inhibitor-loaded micelles 1 day after painful nerve root compression, micelle blood circulation half-life is calculated to be approximately 45 min (Figure S11A). *In vivo* toxicity was also assessed 7 days after intravenous administration of $sPLA_2$ inhibitor-loaded micelles in major organs using histological staining, and no major abnormalities are observed in the heart, liver, spleen, lung, kidney, and brain following micelle administration compared to saline-injected controls (Figure S11B).

In this work, we show that $sPLA_2$ expression after painful injury is significantly increased (Figure 2). This finding suggests that $sPLA_2$ can be a signature of painful tissue and may act as a therapeutic target for neuropathic pain treatment. However, traditional approaches for delivery of anti-inflammatory and neuromodulatory drugs are not very effective for attenuating or abolishing the pain. Drug delivery systems utilizing nanoparticles are

increasingly being used to improve therapeutic delivery owing to their ability to increase the effective drug concentration at sites of inflammation while reducing off-target toxicity.[45] We have recently reported the nanoparticle based on SPIO-loaded phospholipid micelles.[49] In this study, we incorporated the $sPLA_2$ inhibitor TEA-PC into this nanoformulation. These micelle nanoparticles can release their payload based on the pathological conditions by the pain state itself, *i.e.*, different $sPLA_2$ activity and expression. It was found that leveraging the robust neuroinflammation that occurs with painful neuropathy effectively directs the accumulation and release of encapsulated drugs from micelles and provides long-lasting pain relief (Figures 4A and 5A). Capitalizing on increased expression of $sPLA_2$ in the dorsal root ganglia[50] ensures localized release of the inhibitor drug where it can have the most impact on phospholipase activity. Administration of these $sPLA_2$ inhibitor-loaded micelles immediately after compression and directly to the nerve root fully prevents the pain that typically develops after a painful root injury (Figure 4A). However, these studies were only carried out to postoperative day 7, and it is unknown if pain develops in the following weeks. More clinically relevant is the finding that its intravenous delivery after painful neuropathy is already established abolishes existing pain (Figure 5A). The intravenous dose of the $sPLA_2$ inhibitor (0.25 mg/mL) used in these micelles not only was comparable to previous intrathecal doses of PLA_2 inhibitors shown to provide pain relief[51,52] but was also approximately 30 times lower than the oral PLA_2 inhibitor dose and 1000 times lower than the COX-2 inhibitor dose[53,54] needed to attenuate neuropathic pain.[55] Further, unlike many pharmacologic neuropathic pain treatments that require continuous and invasive intrathecal delivery or repeated daily dosing,[53,54] the $sPLA_2$ inhibitor-loaded micelles were effective in fully preventing pain with only a single low dose or only two separate doses to attenuate existing pain. These studies suggest that these targeted drug delivery methods could provide a much-needed solution to the limited efficacy of current neuropathic pain therapeutics. As a platform, $sPLA_2$ inhibitor-loaded micelles could not only remove the need for invasive treatments but increase the therapeutic index of many pain therapeutics that are currently not used in the clinic due to substantial side-effects.

In addition to preventing and abolishing pain, both administration paradigms of $sPLA_2$ inhibitor-loaded micelles also normalize the spinal $sPLA_2$ expression at the C7 spinal level (Figure 4D and Figure 5C), confirming that the active drug is released as observed with the *in vitro* experiments (Figure 3C). This is further corroborated by the >6-fold difference in $sPLA_2$ activity in serum and in the injured spinal cord (Figure S7A), suggesting that greater inhibitor release from micelles occurs at the injured nerve root and spinal cord rather than during circulation. Further, the extent of the decreases in spinal $sPLA_2$ is similar for both administration paradigms (Figure 4D and Figure 5C), suggesting that the systemic administration achieved similar inhibitory activity at the injured spinal level to that of locally administered injections. However, since neither the $sPLA_2$ inhibitor TEA-PC nor the encapsulated TEA-PC readily cross the blood spinal cord barrier (BSCB),[56] it may have trafficked there when the barrier was disrupted, as evidenced by the spinal accumulation of iron oxide particles after painful nerve root compression at day 7 (Figure S9). BSCB breakdown occurs as early as 1 day after spinal cord and radicular injuries but is restored by day 7. Although both treatments may leverage the BSCB being open to meditate $sPLA_2$ in the spinal cord, it is unknown if the same effects would be observed with a later delivery

time. Despite this uncertainty, current neuropathic pain treatments such as morphine and cytokine antagonists, even given as early as day 1 and to the injury site or directly to the spinal cord, fail to completely abolish pain.[57,58] Whether the encapsulated drug relieves pain by acting exclusively in the periphery, spinally, or through a combination of both, the use of $sPLA_2$-responsive phospholipid micelles as a delivery platform ensures the drug's highest possible therapeutic value.

Despite $sPLA_2$'s established role in neuroinflammation,[51,59] few studies have utilized it for pain treatment. Although direct application of $sPLA_2$ to the naïve spinal cord induces pain,[60] most interventions focus on its downstream inflammatory effects, including blocking the COX enzymes, which utilize arachidonic acid for the synthesis of prostaglandins.[60,61] Yet, COX inhibitors and the larger class of nonsteroidal anti-inflammatory drugs (NSAIDs) have limited utility for neuropathic pain since they have substantial renal and cardiovascular toxicities and limited efficacy without daily repeated administration.[62] Further, although other phospholipase A_2 inhibitors reduce pain after neuropathy, analgesia is only transient.[52] Intrathecal administration of the cytosolic phospholipase A_2 inhibitor ($cPLA_2$) AACOCF3 reduces behavioral sensitivity when given 1 day after chronic constriction of the sciatic nerve, but only if given under daily repeated dosing.[45] The differences in dosing between $sPLA_2$ and $cPLA_2$ inhibition may depend on differences between arachidonic acid generation from these two phospholipase A_2 isoforms. *In vitro* activity studies suggest that $cPLA_2$ may have more of a regulatory role in cellular membrane maintenance, whereas $sPLA_2$ may be more responsible for arachidonic acid production and exacerbating downstream inflammatory cascades.[63] Inhibiting $sPLA_2$ decreased the activation of spinal microglia and microglial $sPLA_2$ expression at day 7 (Figure 4E and Figure S10). Since the increased neuroinflammation evident days after injury is responsible for the progression toward persistent neuropathic pain, it is likely that inhibiting $sPLA_2$ in this early window interferes with the establishment of persistent pain altogether.[64] In addition to inflammation, $sPLA_2$ has also been shown to modulate neuronal excitatory transmission[65,66] and may contribute to the heightened neuronal activity that maintains neuropathic pain.[67] In pilot studies with glutamate-stimulated cortical neurons,[66] treatment with TEA-PC reduces neuronal calcium events compared to media vehicle controls by 62.8 ± 13.3%, suggesting that $sPLA_2$ inhibition may reduce the heightened neuronal activity that maintains nerve root-mediated pain.[64] These studies suggest that, mechanistically, $sPLA_2$ may contribute to both the inflammation and increased neuronal activity attributed to persistent neuropathic pain, and probing these mechanisms further would provide better insights into the timing and dosing of these inhibitor micelles for patients.

Although here the repeated dose was needed to attenuate pain (Figure 5A and Figure S8), whether a greater administration dose of $sPLA_2$ inhibitor-loaded micelles on day 1 would provide long-lasting pain relief in a single dose is unknown. Since the systemic dose used to inhibit $sPLA_2$ on days 1 and 2 is sufficient to reduce $sPLA_2$ expression in the spinal cord and DRG at day 7 (Figure 5C and D), early $sPLA_2$ inhibition in both regions may be necessary to attenuate pain. Therefore, further studies are also needed to identify the individual contributions of peripheral and spinal $sPLA_2$ to the progression of persistent pain. Nevertheless, these data together suggest that systemic $sPLA_2$ inhibition may be a potent

alternative to current anti-inflammatory strategies used to manage persistent neuropathic pain.

In this study, the incorporation of the SPIO core into $sPLA_2$ inhibitor-loaded micelles was used to identify accumulation of the micelle *in vivo*. The use of the SPIO core can also be used to detect sites of neuroinflammation[68] as well as localize sites of macrophage infiltration after painful nerve root compression using MR imaging.[17] Therefore, future work seeks to combine drug ($sPLA_2$ inhibitor) and MR imaging agents (SPIOs) in a single nanoformulation. Noninvasive MR imaging could be used for *in vivo* real-time tracking of theranostic micelle accumulation and assessing local pathological states. By combining therapeutics and diagnostic information into a single platform, $sPLA_2$ inhibitor and SPIO-loaded micelles could provide important insights into heterogeneities between pain symptoms and pathologies at the individual patient level, which may be crucial in developing effective treatments for painful neuropathies.[48]

CONCLUSIONS

This study demonstrates that $sPLA_2$-responsive phospholipid micelles provide localized delivery of encapsulated drugs and can even be more efficacious than traditional intrathecal delivery methods for treating chronic pain. Leveraging $sPLA_2$ activity in painful syndromes helps exploit the release of the inhibitor and possibly other drugs locally to the areas that are directly involved in pain, facilitating both pain treatment and possibly image tracking of the active disease state. Given the role of $sPLA_2$ in many different inflammatory and neuropathic pain syndromes,[59,69] $sPLA_2$-responsive phospholipid micelles have a potentially broad reach. Further, this $sPLA_2$ micelle platform can be expanded to encapsulate other drugs including neuromodulatory drugs, which despite success in animal models, have not been adopted into the clinic since systemic administration requires high doses, which induce substantial off-target side-effects. $sPLA_2$ inhibitor-loaded phospholipid micelles may potentially address the clinical challenge of delivering pain therapeutics to achieve long lasting pain relief, without the debilitating off-target toxicities.

METHODS

Materials.

TEA-PC was purchased from Cayman Chemical (Ann Arbor, MI, USA). HSPC, 1,2-distearoyl-*sn*-glycero-3-phosphoethanol-amine-N-[methoxy(polyethylene glycol)-2000] (DSPE-PEG2000), and NBD-PC were purchased from Avanti Polar Lipids, Inc. Secreted phospholipase A_2 enzyme from *Naja mossambica* was purchased from Sigma-Aldrich Co. 3′,3-Diaminobenzidine (DAB) was purchased from Vector Inc. Goat polyclonal antibody to $sPLA_2$-IIA and rabbit polyclonal antibody to Iba1 were purchased from Santa Cruz Biotechnology Inc. and Wako, respectively. All other chemicals were used as received. All of the buffer solutions were prepared with deionized water.

Synthesis of Hydrophobic 7 nm Superparamagnetic Iron Oxide Nanoparticles.

Oleic acid-coated SPIONs were prepared by thermal decomposition as previously described.[49] After allowing the reaction to cool to room temperature, acetone was added and the

sample was centrifuged to precipitate the nanoparticles. The particles were further washed in hexane and precipitated again using acetone followed by centrifugation. This washing procedure was repeated until the supernatant was clear. The particles were then allowed to air-dry and dissolved in toluene at ~40 mg/mL.

Synthesis of PLA_2 Inhibitor and SPION-Loaded Micelles.

$sPLA_2$ inhibitor-loaded micelles were prepared using an oil-in-water emulsion method.[49] A mixture (230 μL) containing HSPC (1 mg in 20 μL of chloroform), PLA_2 inhibitor TEA-PC (1 mg in 100 μL of ethanol), DSPE-PEG2000 (0.25 mg in 10 μL of chloroform), and SPIO NPs (2 mg in 100 μL of toluene) was injected into a glass vial containing 4 mL of water, and the sample was sonicated (Branson Ultrasonics, Danbury, CT, USA) until a homogeneous mixture was achieved. The toluene and chloroform were then allowed to evaporate overnight. $sPLA_2$ inhibitor- and SPION-loaded phospholipid micelle samples were then centrifuged (Eppendorf microcentrifuge 5418) at 1000 rpm for 30 min to remove large aggregates. In order to remove empty micelles, the resulting supernatant was then centrifuged at 10 000 rpm for half an hour, and the pellet was resuspended in water. The stock solution of $sPLA_2$ inhibitor- and SPION-loaded phospholipids micelles was stored in the dark at 4 °C. The unloaded micelles, *i.e.*, without PLA_2 inhibitor, were prepared using similar procedures to the $sPLA_2$ inhibitor- and SPION-loaded phospholipid micelles. Synthesized $sPLA_2$ inhibitor-loaded micelles were incubated in 0.1 M PBS (pH 7.4) for the stability study. DLS was used to monitor the particle size over a total of 1 week.

In Vitro PLA_2 Response Study.

To study the efficiency of cargo release from $sPLA_2$ inhibitor-loaded micelles, the dequenching of NBD-incorporated liposomes incubated with $sPLA_2$ inhibitor-loaded micelles in the presence of $sPLA_2$ enzyme was directly measured. To develop the NBD-incorporated liposomes, a 80 mol % HSPC/20 mol % NBD-PC mixture was prepared in chloroform in a glass vial using a total 1 mg amount of HSPC. The chloroform solvent was removed using a direct stream of nitrogen, prior to vacuum desiccation for a minimum of 4 h. After vacuum desiccation and the formation of a dried lipid film, liposomal samples were then incubated with 0.2 mL in a 50 °C water bath for 0.5 h followed by another 0.5 h of direct sonication at the same temperature to yield the NBD-incorporated liposomes. The stock solution of NBD-incorporated liposomes was stored in the dark at 4 °C.

Dequenching measurements were performed by first preincubating a mixture of either $sPLA_2$ inhibitor-loaded or unloaded micelles with the $sPLA_2$ enzyme (10 μL of $sPLA_2$ inhibitor-loaded [TEA-PC = 0.125 and 0.25 mg/mL] or unloaded micelles + 6.67 μL of $sPLA_2$ enzyme [PLA_2 = 7.5 U/mL]) for 20 min. Fluorescent measurements of the NBD-incorporated liposomes in buffer (20 μL of NBD-incorporated liposomal suspension ([HSPC] = 1 mg/mL) + 0.48 mL of 0.01 M HEPES (pH 7.4) buffer solution containing 2 mM $CaCl_2$) were taken for 5 min prior to the addition of the incubation mixture of the $sPLA_2$ inhibitor-loaded or unloaded micelles. The fluorescence intensity at 520 nm was measured using an excitation at 460 nm. The amount of NBD dequenched (% NBD dequenched) was calculated as $([I_x - I_0]/[I_t - I_0]) \times 100$, where I_0 is the fluorescence intensity of the liposomal suspension containing NBD at the initial time, I_x is the

fluorescence intensity at any given time, and I_t is the fluorescence intensity after addition of 20 μL of Triton X-100 (50 mM) to the suspension at the end of experiment.

In Vitro Cytotoxicity.

To assess *in vitro* cytotoxicity to neural cells, dorsal root ganglia were isolated from embryonic day 18 Sprague–Dawley rats and stored in Hibernate-E medium (Thermo-Scientific, Waltham, MA, USA) supplemented with 2% B-27 and 0.5 mM GlutaMAX (Thermo-Scientific) for 2 days until dissociation. To perform DRG dissociation, Hibernate-E medium was aspirated and DRGs were incubated with warm 0.25% trypsin in EDTA for 1 h at 37 °C. After that, feeding medium (Neurobasal supplemented with 2% B-27, 0.5 mM GlutaMAX, 1% fetal bovine serum (FBS), 0.02 μg/mL nerve growth factor (NGF), 2.5 mg/mL glucose, and 40 μM M2 (5-fluoro-2′-deoxyridine 10 mM, uridine 10 mM) with an additional 5% FBS was added to inhibit trypsin activity. DRGs were then manually titurated with a pestle, centrifuged at 1000 rpm for 5 min at room temperature, isolated from their supernatant, and then reconstituted with fresh feeding medium. Dissociated DRGs were then plated (3.97×10^6 cells/mL) onto a 24-well plastic tissue culture plate treated with poly-D-lysine (PDL) and laminin. Feeding medium was changed at day *in vitro* (DIV) 1 and DIV 3. On DIV 4, cultures were separately incubated for 24 h with micelles at different PLA_2 inhibitor concentrations: 0, 1, 5, 10, 20, 50, 100, 200, and 250 μg/mL. Cell viability was tested in triplicate for each concentration using a CellTiter 96 AQ One Solution cell proliferation assay (Promega, Madison, WI, USA). Cytotoxicity measurements from treated groups were normalized to untreated controls as previously described.[70,71] Average percent cell viability was compared using a one-way ANOVA (group) with Tukey's test.

In Vivo Injury and $sPLA_2$ Inhibitor-Loaded Micelles Administration.

All studies were approved by our Institutional Animal Care and Use Committee and carried out under the guidelines of the Committee for Research and Ethical Issues of the International Association for the Study of Pain. First, spinal $sPLA_2$ expression was characterized after a painful root injury. As such, rats underwent either a nerve root compression that was painful (15 min; $n = 11$) or a compression that served as a control since it was nonpainful (3 min; $n = 11$); sham injuries ($n = 10$) were also included as surgical controls. Under isoflurane anesthesia (4% induction, 2% maintenance), male Holtzman rats underwent a painful nerve root compression in which the right C7 nerve root was surgically exposed and compressed for 15 min with a 10*g* force microvascular clip as previously described.[64]

To test the effectiveness of $sPLA_2$ inhibitor-loaded micelles in preventing the pain that develops from a neuropathic injury, $sPLA_2$ inhibitor-loaded micelles were administered *in vivo* after a painful nerve root compression.[64] Immediately after tissue compression, two separate groups of rats received either 100 μL (TEA-PC concentration: 0.25 mg/mL) of $sPLA_2$ inhibitor-loaded micelles in saline ($sPLA_2$ inhibitor-loaded micelles; $n = 5$) or a comparable dose of control micelles without any $sPLA_2$ inhibitor loaded in saline (unloaded micelles; $n = 3$) administered directly to the nerve root. After each surgery, incisions were closed using 3–0 polyester sutures and surgical staples, and the rats were monitored during recovery in room air.

To assess if the same dose of inhibitor micelles that were effective in preventing pain with local administration could be as effective when administered systemically, in a pilot study ($sPLA_2$ inhibitor-loaded micelles; $n = 4$), rats received 100 μL of $sPLA_2$ inhibitor-loaded micelles (TEA-PC concentration: 0.25 mg/mL) diluted in PBS that were administered *via* tail vein only on day 1 after a painful nerve root compression. In a second study, separate groups of rats received either 100 μL of $sPLA_2$ inhibitor-loaded micelles (TEA-PC concentration: 0.25 mg/mL), $sPLA_2$ (inhibitor-loaded micelles, $n = 5$) or a comparable dose of unloaded control micelles (unloaded micelles; $n = 4$) diluted in 400 μL of PBS administered intravenously through the tail vein after the nerve root compression on both day 1 and day 2.[17] Additional groups of rats were included as sham-surgical controls (sham + $sPLA_2$ inhibitor-loaded micelles; $n = 4$) in which rats received identical surgical procedures in which the nerve root was exposed but not compressed.

Behavior Testing for Pain Sensitivity.

Behavioral sensitivity following either micelle administration paradigm (local: $sPLA_2$ inhibitor-loaded micelles; $n = 5$; unloaded micelles; $n = 3$; and intravenous: $sPLA_2$ inhibitor-loaded micelles; $n = 5$; unloaded micelles; $n = 4$) was assessed by measuring the bilateral forepaw withdrawal threshold to mechanical stimulation, using a modified Chaplan's up–down method.[64] Testing was performed at baseline before injury (day 0) and daily for 7 days after and was quantified as the paw withdrawal threshold to an applied mechanical stimulus. Rats were randomly placed into different test chambers and allowed to acclimate for 20 min prior to testing. The thresholds for eliciting a withdrawal response were quantified by stimulating each forepaw using a series of von Frey filaments (Stoelting; Wood Dale, IL, USA) with increasing strengths (1.4, 2, 4, 6, 8, 15, and 26 gf). An observer, blinded to the group, applied each filament five times before advancing to the next highest strength, and if two consecutive filaments both induced a withdrawal response, the lower strength filament was recorded as the threshold. The withdrawal threshold was taken as the lowest von Frey filament to elicit a response and was confirmed by the next filament also provoking a response.[72] Testing sessions consisted of 3 rounds each separated by 10 min of rest. The withdrawal thresholds were separately averaged across rounds for each day, and differences in thresholds between groups were compared separately for the ipsilateral and contralateral forepaw using a repeated-measures ANOVA with *posthoc* Tukey's test. No rats were excluded from behavioral testing or analysis.

Tissue Harvest, Prussian Blue Staining, and Immunohis-tochemistry.

For the studies characterizing $sPLA_2$ expression in the bilateral spinal cord, tissue at the C7 level was separately harvested on days 1 (painful $n = 6$; nonpainful $n = 5$; sham $n = 5$) and day 7 (painful $n = 5$; nonpainful $n = 6$; sham $n = 5$). For all micelle treatment groups, on postoperative day 7 after behavior testing, the C7 nerve roots, DRG, and spinal cord were harvested for histology and immunolabeling. Rats were deeply anesthetized with sodium pentobarbital (65 mg/kg) and transcardially perfused with phosphate-buffered saline (PBS) followed by 4% paraformaldehyde. Sub-sequently, all neural tissues were postfixed in 4% paraformaldehyde overnight, cryoprotected in 30% sucrose, and embedded in OCT medium (VWR, Bridgeport, NJ, USA). All nerve root, DRG, and spinal cord tissues were cryosectioned along the long axis at 14 μm and thaw-mounted onto slides.

For spinal $sPLA_2$ characterization studies, both ipsilateral and contralateral C7 spinal sections were blocked using 10% normal donkey serum (Vector, Burlingame, CA, USA) with 0.3% Triton-X 100 and incubated in goat anti-$sPLA_2$ IIA (1:500; Santa Cruz, Dallas TX, USA). In a separate run, spinal tissue sections were colabeled separately with $sPLA_2$ IIA and mouse-anti MAP2 (1:250; Covance; Cumberland, VA, USA), rabbit anti-Iba1 (1:1000, Wako, Osaka), and rabbit anti-GFAP (1:500; Millipore; Billerca, MA, USA) to label for neuronal, microglial, and astrocytic $sPLA_2$, respectively Tissue sections were then rinsed with PBS and incubated for 2 h at room temperature in either donkey anti-goat 488, donkey anti-mouse 555, or donkey anti-rabbit 546 (1:500, Invitrogen, Carlsbad CA, USA) secondary antibodies. For each rat, 3–6 spinal cord sections were captured using a Leica DM6000 (Wetzlar, Germany) with deconvolution at 20×, and both ipsilateral and contralateral images were cropped to 750 × 200 pixels^2 to contain the superficial (I and II) laminae of the spinal cord dorsal horn. A custom densitometry MATLAB script (Mathworks, Natick, MA, USA) was used to quantify the extent of positive spinal $sPLA_2$, and spinal cord sections from naïve rats ($n = 2$) were acquired and used to set the pixel intensity thresholds used to quantify positive labeling for $sPLA_2$. The ipsilateral expression of total spinal $sPLA_2$ was presented as a fold change over contralateral expression. To quantify colocalization of spinal $sPLA_2$ in neurons, microglia, and astrocytes, the total number of pixels positive for $sPLA_2$ and either MAP2, Iba1, or GFAP is divided by the total number of pixels positive for $sPLA_2$ for each image in the ipsilateral dorsal horn. Spinal neuronal, microglia, and astrocytic $sPLA_2$ and total spinal $sPLA_2$ were compared across groups using a one-way ANOVA with Tukey's *posthoc* test.

To determine the expression of $sPLA_2$ and the extent of Iba1 positive microglia in the spinal cord and $sPLA_2$ expression in the DRG after micelle treatment, sections were similarly blocked and incubated in goat anti-$sPLA_2$ IIA (1:500; Santa Cruz) and rabbit anti-Iba1 (1:1000, Wako, Osaka Japan) primary antibodies as well as donkey anti-goat 488 and donkey anti-rabbit 546 (1:500, Invitrogen) secondary antibodies. Spinal sections were similarly imaged using a Leica DM6000 and cropped to only include the superficial dorsal horn for analysis. Images of the DRG were cropped (450 × 450 pixels) to include 10–20 random neurons per image for intensity analysis. A custom densitometry MATLAB script (Mathworks) was used to quantify the extent of positive spinal $sPLA_2$ and Iba1 labeling and $sPLA_2$ labeling in the DRG, as previously described.[73,74] DRG and spinal cord sections from naïve rats ($n = 2$) were acquired and used to set the pixel intensity thresholds used to quantify positive labeling for $sPLA_2$ and Iba1 separately. Spinal microglial $sPLA_2$ expression after micelle treatment was also evaluated through quantifying the colocalization of $sPLA_2$ and Iba1 labeling as performed in earlier spinal $sPLA_2$ characterization studies. The number of pixels positive for either $sPLA_2$ or Iba1 was calculated as a percent of the total dorsal horn area for each label. Similarly, the positive pixels for $sPLA_2$ were evaluated over the area of selected DRG neurons and compared across groups using a one-way ANOVA with Tukey's *posthoc* test. Total levels of each of $sPLA_2$, Iba1, or microglial $sPLA_2$ labeling were then separately compared to the normal levels and expressed as a fold-change over normal levels for each rat. Differences in normalized intensity between the $sPLA_2$ inhibitor-loaded micelles and the unloaded micelles were compared using separate Student's *t* tests for each label in the spinal cord.

To assess micelle localization, Prussian Blue staining was used to detect SPIONs *via* iron oxide staining.[17] An additional group of naive rats that received no surgery, but the same intravenous dose of $sPLA_2$ inhibitor-loaded micelles (normal + $sPLA_2$ inhibitor-loaded micelles; $n = 2$), was included as histological controls. Nerve root and spinal cord sections were incubated with 0.3% hydrogen peroxide in PBS and a 1:1 mixture of 2% potassium ferrocyanide and 2% hydrochloric acid for 30 min. Visualization of iron in the tissue was enhanced by DAB (Vector) for an additional 15 min. Tissue sections were then counterstained with eosin (Sigma-Aldrich, St. Louis, MO, USA), cleared with xylene (Sigma-Aldrich), and coverslipped using DPX mounting media (Sigma-Aldrich). Spinal sections were imaged using an Olympus 5XB1 microscope (Olympus, Tokyo, Japan).

Pharmacokinetic and *In Vivo* Toxicity Experiments.

Blood circulation of micelles was tested in a separate group of rats ($n = 3$) that received a painful nerve root compression followed by injection of dye-incorporated $sPLA_2$ inhibitor-loaded micelles 1 day after injury *via* tail vein injections. Dye-loaded $sPLA_2$ inhibitor-loaded micelles were fabricated by incorporating 10 mol % rhodamine-PE during the micelle preparation. One day after painful nerve root injury, rats received 500 μL of the dye-loaded $sPLA_2$ inhibitor-loaded micelles (TEA-PC; 0.5 mg/mL) diluted in saline. Whole blood samples were collected in heparinized tubes at baseline prior to injection (0 h) and then 0.5, 1, 2, 4, 8, 12, and 24 h after injection. Fluorescence spectra of rhodamine from blood samples were collected by a FluoroMax-3 spectrofluorimeter (Horiba Jobin Yvon, Edison, NJ, USA). For *in vivo* toxicity studies, tissue from the same group of rats was harvested with fresh PBS at day 7, and major organs were postfixed in 4% paraformaldehyde for 48 h. A second group of rats ($n = 2$) that did not receive surgery but did receive an intravenous injection of 500 μL of saline was included as histological controls. Organ tissue was then prepared for paraffin embedding and sectioned serially at a 6 μm thickness across the entire organ. Tissue sections were then stained with hematoxylin and eosin (H&E) to assess cellular and tissue architecture as previously described.[75]

$sPLA_2$ Activity Assay and Circulating $sPLA_2$ Experiment.

To assess if circulating $sPLA_2$ in blood affects inhibitor release from $sPLA_2$ inhibitor-loaded micelles, both blood and spinal cord tissue were collected from rats 1 day after receiving a painful nerve root compression and assayed using an $sPLA_2$ activity kit from Cayman Chemical (Ann Arbor, MI, USA). In a subset of rats ($n = 3$) that received only a painful nerve root compression, serum samples were collected from whole blood samples as previously described.[65] Blood was collected from the tail vein before surgery and 1 day after surgery and centrifuged to separate the serum from other whole-blood components. At the same time point, ipsilateral C7 spinal cord also was collected, flash frozen, and stored at −70 °C until assayed. Spinal cords at the C7 level from naïve uninjured rats ($n = 2$) were also harvested as controls. Both serum and spinal cord samples were assayed for $sPLA_2$ activity as per the kit instructions. Activity measurement from injured serum was normalized to each rat's baseline (prior to compression injury), and spinal cord activity was normalized to naïve spinal cord measurements. Both serum and spinal cord $sPLA_2$ activity were compared to each other using Student's *t* test.

Serum samples were also used to test liposomal integrity in the presence of circulating $sPLA_2$ enzymes *in vitro*. In separate studies, 30 μL of an NBD-incorporated liposomal suspension in 10 mM HEPES (2 mM $CaCl_2$, pH 7.4) was first mixed with 30 μL of serum from healthy or injured rats. Either immediately after mixing or after 24 h of incubation, 20 μL of the mixture was added to 480 μL of HEPES buffer and fluorescent measurements were taken. Fluorescent intensity measurements were acquired using a single excitation at 460 nm. The fluorescent emission was collected from 490 to 580 nm. At the end of the experiment, total NBD fluorescence was determined by the addition of Triton X-100. The fluorescence intensity was then normalized relative to the intensity of the Triton-treated sample at 540 nm.

Instrumentation.

Fluorescence spectra measurements were made on a SPEX FluoroMax-3 spectrofluorometer (Horiba Jobin Yvon). DLS measurements were performed on a Zetasizer Nano (Malvern Instruments). The scattering angle was held constant at 90°. Transmission electron microscopy (JEM-1010) was used to characterize the size and shape of the small hydrophobic SPION and SPION-loaded phospholipid micelles. T_2 relaxation times were determined using a Bruker mq60 MR relaxometer operating at 1.41 T (60 MHz). The Fe concentration in samples was determined by ICP-OES analysis using a Genesis ICPOES (Spectro Analytical Instruments GMBH; Kleve, Germany).

Supplementary Material

Refer to Web version on PubMed Central for supplementary material.

ACKNOWLEDGMENTS

This work was supported in part by the National Institutes of Health R01NS100892 (Z.C.), the Cervical Spine Research Society, Catherine Sharpe Foundation, and the PENN ITMAT-CT3N Pilot Project.

REFERENCES

(1). DiBonaventura MD; Sadosky A; Concialdi K; Hopps M; Kudel I; Parsons B; Cappelleri JC; Hlavacek P; Alexander AH; Stacey BR; Markman JD; Farrar JT The Prevalence of Probable Neuropathic Pain in the Us: Results from a Multimodal General-Population Health Survey. J. Pain Res 2017, 10, 2525–2538. [PubMed: 29138590]

(2). Scholz J; Woolf CJ The Neuropathic Pain Triad: Neurons. Nat. Neurosci 2007, 10, 1361–1368. [PubMed: 17965656]

(3). Moalem G; Tracey DJ Immune and Inflammatory Mechanisms in Neuropathic Pain. Brain Res. Rev 2006, 51, 240–264. [PubMed: 16388853]

(4). Harden N; Cohen M Unmet Needs in the Management of Neuropathic Pain. J. Pain Symptom Manage 2003, 25, S12–17. [PubMed: 12694988]

(5). Radhakrishnan K; Litchy WJ; O'Fallon WM; Kurland LT Epidemiology of Cervical Radiculopathy. A Population-Based Study from Rochester, Minnesota, 1976 through 1990. Brain 1994, 117, 325–335. [PubMed: 8186959]

(6). Waters TR National Efforts to Identify Research Issues Related to Prevention of Work-Related Musculoskeletal Disorders. J. Electromyogr. Kinesiol 2004, 14, 7–12. [PubMed: 14759745]

(7). Cote P; Cassidy JD; Carroll LJ; Kristman V The Annual Incidence and Course of Neck Pain in the General Population: A Population-Based Cohort Study. Pain 2004, 112, 267–273. [PubMed: 15561381]

(8). Gilron I; Baron R; Jensen T Neuropathic Pain: Principles of Diagnosis and Treatment. Mayo Clin. Proc 2015, 90, 532–545. [PubMed: 25841257]

(9). Henschke N; Kamper SJ; Maher CG The Epidemiology and Economic Consequences of Pain. Mayo Clin. Proc 2015, 90, 139–147. [PubMed: 25572198]

(10). Chizh BA; Headley PM Nmda Antagonists and Neuropathic Pain - Multiple Drug Targets and Multiple Uses. Curr. Pharm. Des 2005, 11, 2977–2994. [PubMed: 16178757]

(11). McNicol ED; Midbari A; Eisenberg E Opioids for Neuropathic Pain. Cochrane Database Syst. Rev 2013, 8, Cd006146.

(12). Moore RA; Chi CC; Wiffen PJ; Derry S; Rice AS Oral Nonsteroidal Anti-Inflammatory Drugs for Neuropathic Pain. Cochrane Database Syst. Rev 2015, 10, Cd010902.

(13). Dworkin RH; O'Connor AB; Audette J; Baron R; Gourlay GK; Haanpaa ML; Kent JL; Krane EJ; Lebel AA; Levy RM; Mackey SC; Mayer J; Miaskowski C; Raja SN; Rice AS; Schmader KE; Stacey B; Stanos S; Treede RD; Turk DC; et al. Recommendations for the Pharmacological Management of Neuropathic Pain: An Overview and Literature Update. Mayo Clin. Proc 2010, 85, S3–14.

(14). Trbovich M; Yang H Capsaicin 8% Patch for Central and Peripheral Neuropathic Pain of Persons with Incomplete Spinal Cord Injury: Two Case Reports. Am. J. Phys. Med. Rehabil 2015, 94, e66–72. [PubMed: 26035723]

(15). Rothman SM; Winkelstein BA Chemical and Mechanical Nerve Root Insults Induce Differential Behavioral Sensitivity and Glial Activation That Are Enhanced in Combination. Brain Res. 2007, 1181, 30–43. [PubMed: 17920051]

(16). Kelly J. D. t.; Aliquo D; Sitler MR; Odgers C; Moyer RA Association of Burners with Cervical Canal and Foraminal Stenosis. Am. J. Sports Med 2000, 28, 214–217. [PubMed: 10750998]

(17). Thorek DL; Weisshaar CL; Czupryna JC; Winkelstein BA; Tsourkas A Superparamagnetic Iron Oxide-Enhanced Magnetic Resonance Imaging of Neuroinflammation in a Rat Model of Radicular Pain. Mol. Imaging 2011, 10, 206–214. [PubMed: 21496449]

(18). Znaor L; Lovric S; Hogan Q; Sapunar D Association of Neural Inflammation with Hyperalgesia Following Spinal Nerve Ligation. Croat. Med. J 2007, 48, 35–42. [PubMed: 17309137]

(19). Hashizume H; DeLeo JA; Colburn RW; Weinstein JN Spinal Glial Activation and Cytokine Expression after Lumbar Root Injury in the Rat. Spine (Philadelphia) 2000, 25, 1206–1217.

(20). Winkelstein BA; DeLeo JA Nerve Root Injury Severity Differentially Modulates Spinal Glial Activation in a Rat Lumbar Radiculopathy Model: Considerations for Persistent Pain. Brain Res. 2002, 956, 294–301. [PubMed: 12445698]

(21). DeLeo JA; Yezierski RP The Role of Neuroinflammation and Neuroimmune Activation in Persistent Pain. Pain 2001, 90, 1–6. [PubMed: 11166964]

(22). Sweitzer SM; Hickey WF; Rutkowski MD; Pahl JL; DeLeo JA Focal Peripheral Nerve Injury Induces Leukocyte Trafficking into the Central Nervous System: Potential Relationship to Neuropathic Pain. Pain 2002, 100, 163–170. [PubMed: 12435469]

(23). Watkins LR; Milligan ED; Maier SF Spinal Cord Glia: New Players in Pain. Pain 2001, 93, 201–205. [PubMed: 11514078]

(24). Rutkowski MD; Pahl JL; Sweitzer S; van Rooijen N; DeLeo JA Limited Role of Macrophages in Generation of Nerve Injury-Induced Mechanical Allodynia. Physiol. Behav 2000, 71, 225–235. [PubMed: 11150554]

(25). Rutkowski MD; Winkelstein BA; Hickey WF; Pahl JL; DeLeo JA Lumbar Nerve Root Injury Induces Central Nervous System Neuroimmune Activation and Neuroinflammation in the Rat: Relationship to Painful Radiculopathy. Spine 2002, 27, 1604–1613. [PubMed: 12163719]

(26). Winkelstein BA; Rutkowski MD; Sweitzer SM; Pahl JL; DeLeo JA Nerve Injury Proximal or Distal to the Drg Induces Similar Spinal Glial Activation and Selective Cytokine Expression but Differential Behavioral Responses to Pharmacologic Treatment. J. Comp. Neurol 2001, 439, 127–139. [PubMed: 11596043]

(27). Watkins LR; Wiertelak EP; Goehler LE; Smith KP; Martin D; Maier SF Characterization of Cytokine-Induced Hyperalgesia. Brain Res. 1994, 654, 15–26. [PubMed: 7982088]

(28). Latremoliere A; Woolf CJ Central Sensitization: A Generator of Pain Hypersensitivity by Central Neural Plasticity. J. Pain 2009, 10, 895–926. [PubMed: 19712899]

(29). Zhao Z; Liu N; Huang J; Lu PH; Xu XM Inhibition of Cpla2 Activation by Ginkgo Biloba Extract Protects Spinal Cord Neurons from Glutamate Excitotoxicity and Oxidative Stress-Induced Cell Death. J. Neurochem 2011, 116, 1057–1065. [PubMed: 21182525]

(30). Toborek M; Malecki A; Garrido R; Mattson MP; Hennig B; Young B Arachidonic Acid-Induced Oxidative Injury to Cultured Spinal Cord Neurons. J. Neurochem 1999, 73, 684–692. [PubMed: 10428065]

(31). Miyamoto H; Saura R; Harada T; Doita M; Mizuno K The Role of Cyclooxygenase-2 and Inflammatory Cytokines in Pain Induction of Herniated Lumbar Intervertebral Disc. Kobe J. Med. Sci 2000, 46, 13–28. [PubMed: 11193500]

(32). Carabaza A; Cabre F; Garcia AM; Gomez M; Sanchez J; Mauleon D; Carganico G Inhibition of Phospholipase A2 Purified from Human Herniated Disc. Biochem. Pharmacol 1993, 45, 783–786. [PubMed: 8442777]

(33). Biyani A; Andersson GB Low Back Pain: Pathophysiology and Management. J. Am. Acad. Orthop. Surg 2004, 12, 106–115. [PubMed: 15089084]

(34). Franson RC; Saal JS; Saal JA Human Disc Phospholipase A2 Is Inflammatory. Spine (Philadelphia) 1992, 17, S129–132.

(35). Piperno M; Hellio le Graverand MP; Reboul P; Mathieu P; Tron AM; Perrin G; Peschard MJ; Richard M; Vignon E Phospholipase A2 Activity in Herniated Lumbar Discs. Clinical Correlations and Inhibition by Piroxicam. Spine (Philadelphia) 1997, 22, 2061–2065.

(36). Kawakami M; Tamaki T; Hayashi N; Hashizume H; Nishi H Possible Mechanism of Painful Radiculopathy in Lumbar Disc Herniation. Clin. Orthop. Relat. Res 1998, 351, 241–251.

(37). Kishimoto K; Matsumura K; Kataoka Y; Morii H; Watanabe Y Localization of Cytosolic Phospholipase A2Messenger Rna Mainly in Neurons in the Rat Brain. Neuroscience 1999, 92, 1061–1077. [PubMed: 10426546]

(38). Ong WY; Horrocks LA; Farooqui AA Immunocy-tochemical Localization of Cpla2 in Rat and Monkey Spinal Cord. J. Mol. Neurosci 1999, 12, 123–130. [PubMed: 10527456]

(39). Murakami M; Nakatani Y; Atsumi G; Inoue K; Kudo I Regulatory Functions of Phospholipase A2. Crit. Rev. Immunol 1997, 17, 225–283. [PubMed: 9202883]

(40). van Rossum GS; Drummen GP; Verkleij AJ; Post JA; Boonstra J Activation of Cytosolic Phospholipase A2 in Her14 Fibroblasts by Hydrogen Peroxide: A P42/44(Mapk)-Dependent and Phosphorylation-Independent Mechanism. Biochim. Biophys. Acta, Mol. Cell Biol. Lipids 2004, 1636, 183–195.

(41). Klein J Membrane Breakdown in Acute and Chronic Neurodegeneration: Focus on Choline-Containing Phospholipids. J. Neural Transm 2000, 107, 1027–1063. [PubMed: 11041281]

(42). Sun GY; Xu JF; Jensen MD; Simonyi A Phospholipase a(2) in the Central Nervous System: Implications for Neuro-degenerative Diseases. J. Lipid Res 2004, 45, 205–213. [PubMed: 14657205]

(43). Tang ZY; Shu B; Cui XJ; Zhou CJ; Shi Q; Holz J; Wang YJ Changes of Cervical Dorsal Root Ganglia Induced by Compression Injury and Decompression Procedure: A Novel Rat Model of Cervical Radiculoneuropathy. J. Neurotrauma 2009, 26, 289–295. [PubMed: 19191544]

(44). Osikowicz M; Mika J; Przewlocka B The Glutamatergic System as a Target for Neuropathic Pain Relief. Exp. Physiol 2013, 98, 372–384. [PubMed: 23002244]

(45). Wilczewska AZ; Niemirowicz K; Markiewicz KH; Car H Nanoparticles as Drug Delivery Systems. Pharmacol. Rep 2012, 64, 1020–1037. [PubMed: 23238461]

(46). Xin Y; Huang M; Guo WW; Huang Q; Zhang LZ; Jiang G Nano-Based Delivery of RNAi in Cancer Therapy. Mol. Cancer 2017, 16, 1–9. [PubMed: 28093071]

(47). Cheng Z; Al Zaki A; Hui JZ; Muzykantov VR; Tsourkas A Multifunctional Nanoparticles: Cost *Versus* Benefit of Adding Targeting and Imaging Capabilities. Science 2012, 338, 903–910. [PubMed: 23161990]

(48). Finnerup NB; Attal N; Haroutounian S; McNicol E; Baron R; Dworkin RH; Gilron I; Haanpaa M; Hansson P; Jensen TS; Kamerman PR; Lund K; Moore A; Raja SN; Rice AS; Rowbotham M; Sena E; Siddall P; Smith BH; Wallace M Pharmacotherapy for Neuropathic Pain in Adults: A Systematic Review and Meta-Analysis. Lancet Neurol. 2015, 14, 162–173. [PubMed: 25575710]

(49). Gao Q; Yan L; Chiorazzo M; Delikatny EJ; Tsourkas A; Cheng Z Pla2-Responsive and Spio-Loaded Phospholipid Micelles. Chem. Commun. (Cambridge, U. K.) 2015, 51, 12313–12315.

(50). Kartha S; Weisshaar CL; Philips BH; Winkelstein BA Pre-Treatment with Meloxicam Prevents the Spinal Inflammation and Oxidative Stress in Drg Neurons That Accompany Painful Cervical Radiculopathy. Neuroscience 2018, 388, 393–404. [PubMed: 30086368]

(51). Ma L; Uchida H; Nagai J; Inoue M; Aoki J; Ueda H Evidence for De Novo Synthesis of Lysophosphatidic Acid in the Spinal Cord through Phospholipase a(2) and Autotaxin in Nerve Injury-Induced Neuropathic Pain. J. Pharmacol. Exp. Ther 2010, 333, 540–546. [PubMed: 20123931]

(52). Sung B; Wang S; Zhou B; Lim G; Yang L; Zeng Q; Lim JA; Wang JD; Kang JX; Mao J Altered Spinal Arachidonic Acid Turnover after Peripheral Nerve Injury Regulates Regional Glutamate Concentration and Neuropathic Pain Behaviors in Rats. Pain 2007, 131, 121–131. [PubMed: 17267128]

(53). Wang Y; Zhang XA; Guo QL; Zou WY; Huang CS; Yan JQ Cyclooxygenase Inhibitors Suppress the Expression of P2x(3) Receptors in the Drg and Attenuate Hyperalgesia Following Chronic Constriction Injury in Rats. Neurosci. Lett 2010, 478, 77–81. [PubMed: 20450958]

(54). Schafers M; Marziniak M; Sorkin LS; Yaksh TL; Sommer C Cyclooxygenase Inhibition in Nerve-Injury- and Tnf-Induced Hyperalgesia in the Rat. Exp. Neurol 2004, 185, 160–168. [PubMed: 14697327]

(55). Khan M; Shunmugavel A; Dhammu TS; Matsuda F; Singh AK; Singh I Oral Administration of Cytosolic Pla2 Inhibitor Arachidonyl Trifluoromethyl Ketone Ameliorates Cauda Equina Compression Injury in Rats. J. Neuroinflammation 2015, 12, 1–12.

(56). Pardridge WM Drug Transport across the Blood-Brain Barrier. J. Cereb. Blood Flow Metab 2012, 32, 1959–1972. [PubMed: 22929442]

(57). Hook MA; Moreno G; Woller S; Puga D; Hoy K; Balden R; Grau JW Intrathecal Morphine Attenuates Recovery of Function after a Spinal Cord Injury. y 2009, 26, 741–752.

(58). Rothman SM; Winkelstein BA Cytokine Antagonism Reduces Pain and Modulates Spinal Astrocytic Reactivity after Cervical Nerve Root Compression. Ann. Biomed. Eng 2010, 38, 2563–2576. [PubMed: 20309734]

(59). Titsworth WL; Cheng XX; Ke Y; Deng LX; Burckardt KA; Pendleton C; Liu NK; Shao H; Cao QL; Xu XM Differential Expression of Spla(2) Following Spinal Cord Injury and a Functional Role for Spla(2)-Iia in Mediating Oligodendrocyte Death. Glia 2009, 57, 1521–1537. [PubMed: 19306380]

(60). Chacur M; Milligan ED; Sloan EM; Wieseler-Frank J; Barrientos RM; Martin D; Poole S; Lomonte B; Gutierrez JM; Maier SF; Cury Y; Watkins LR Snake Venom Phospholipase A2s (Asp49 and Lys49) Induce Mechanical Allodynia Upon Peri-Sciatic Administration: Involvement of Spinal Cord Glia, Proin-flammatory Cytokines and Nitric Oxide. Pain 2004, 108, 180–191. [PubMed: 15109522]

(61). Ma WY; Du W; Eisenach JC Role for Both Spinal Cord Cox-1 and Cox-2 in Maintenance of Mechanical Hypersensitivity Following Peripheral Nerve Injury. Brain Res. 2002, 937, 94–99. [PubMed: 12020867]

(62). Galluzzi KE Management of Neuropathic Pain. J. Am. Osteopath. Assoc 2005, 105, S12–19.

(63). Han WK; Sapirstein A; Hung CC; Alessandrini A; Bonventre JV Cross-Talk between Cytosolic Phospholipase a(2)Alpha (Cpla(2 Alpha)) and Secretory Phospholipase a(2) (Spla(2)) in Hydrogen Peroxide-Induced Arachidonic Acid Release in Murine Mesangial Cells - Spla(2) Regulates Cpla(2)Alpha Activity That Is Responsible for Arachidonic Acid Release. J. Biol. Chem 2003, 278, 24153–24163. [PubMed: 12676927]

(64). Smith JR; Galie PA; Slochower DR; Weisshaar CL; Janmey PA; Winkelstein BA Salmon-Derived Thrombin Inhibits Development of Chronic Pain through an Endothelial Barrier Protective Mechanism Dependent on Apc. Biomaterials 2016, 80, 96–105. [PubMed: 26708087]

(65). Kolko M; de Turco EB; Diemer NH; Bazan NG Secretory Phospholipase A2-Mediated Neuronal Cell Death Involves Glutamate Ionotropic Receptors. NeuroReport 2002, 13, 1963–1966. [PubMed: 12395100]

(66). DeCoster MA; Lambeau G; Lazdunski M; Bazan NG Secreted Phospholipase A2 Potentiates Glutamate-Induced Calcium Increase and Cell Death in Primary Neuronal Cultures. J. Neurosci. Res 2002, 67, 634–645. [PubMed: 11891776]

(67). D'Mello R; Dickenson AH Spinal Cord Mechanisms of Pain. Br. J. Anaesth 2008, 101, 8–16. [PubMed: 18417503]

(68). Stoll G; Bendszus M New Approaches to Neuroimaging of Central Nervous System Inflammation. Curr. Opin. Neurol 2010, 23, 282–286. [PubMed: 20168228]

(69). Svensson CI; Lucas KK; Hua XY; Powell HC; Dennis EA; Yaksh TL Spinal Phospholipase a(2) in Inflammatory Hyperalgesia: Role of the Small, Secretory Phospholipase a(2). Neuroscience 2005, 133, 543–553. [PubMed: 15885922]

(70). Chan FK; Moriwaki K; De Rosa MJ Detection of Necrosis by Release of Lactate Dehydrogenase Activity. Methods Mol. Biol 2013, 979, 65–70. [PubMed: 23397389]

(71). Prabhu BM; Ali SF; Murdock RC; Hussain SM; Srivatsan M Copper Nanoparticles Exert Size and Concentration Dependent Toxicity on Somatosensory Neurons of Rat. Nano-toxicology 2010, 4, 150–160.

(72). Chaplan SR; Bach FW; Pogrel JW; Chung JM; Yaksh TL Quantitative Assessment of Tactile Allodynia in the Rat Paw. J. Neurosci. Methods 1994, 53, 55–63. [PubMed: 7990513]

(73). Nicholson KJ; Guarino BB; Winkelstein BA Transient Nerve Root Compression Load and Duration Differentially Mediate Behavioral Sensitivity and Associated Spinal Astrocyte Activation and Mglur5 Expression. Neuroscience 2012, 209, 187–195. [PubMed: 22387561]

(74). Zeeman ME; Kartha S; Winkelstein BA Whole-Body Vibration Induces Pain and Lumbar Spinal Inflammation Responses in the Rat That Vary with the Vibration Profile. J. Orthop. Res 2016, 34, 1439–1446. [PubMed: 27571442]

(75). Kartha S; Zeeman ME; Baig HA; Guarino BB; Winkelstein BA Upregulation of BDNF and NGF in Cervical Intervertebral Discs Exposed to Painful Whole-Body Vibration. Spine (Philadelphia) 2014, 39, 1542–1548.

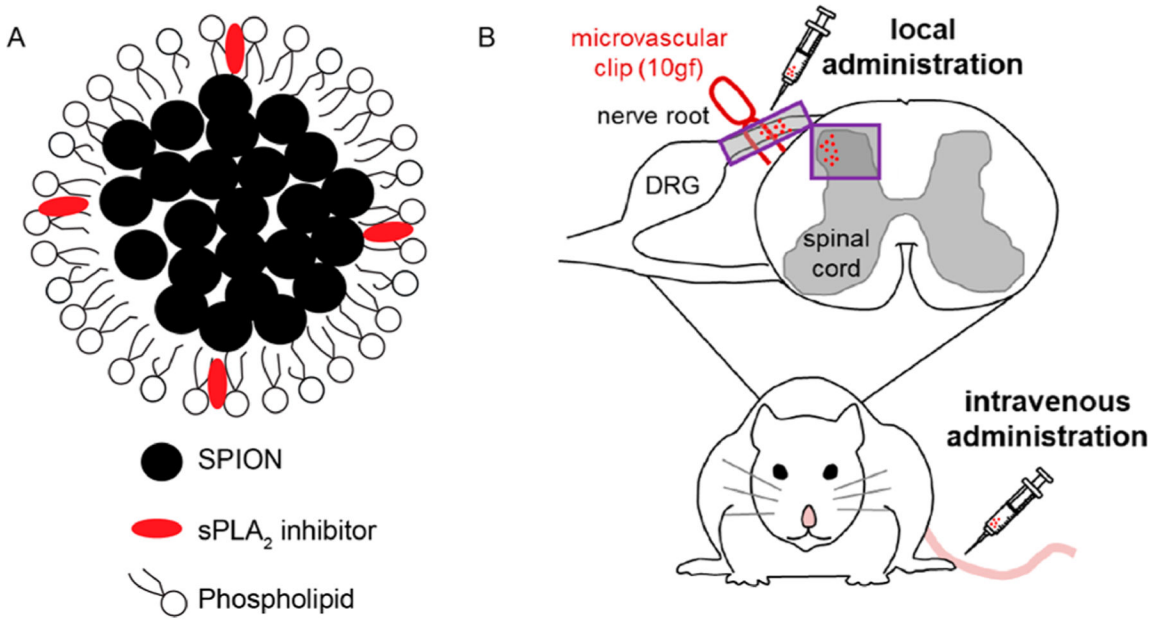

Figure 1.

Schematic diagrams of $sPLA_2$ inhibitor-loaded micelles and their administration following a painful nerve root compression. (A) $sPLA_2$ inhibitor-loaded micelles were formed through the coassembly of the phospholipid and the small hydrophobic SPIO nanoparticles. $sPLA_2$ inhibitor was incorporated into the phospholipid membrane during the micelle preparation. (B) Nerve root compression injury was performed using a microvascular clip (10 gf for 15 min) applied to the right C7 dorsal nerve root. $sPLA_2$ inhibitor-loaded micelles or control unloaded micelles were injected directly onto the nerve root ipsilateral to injury or given by intravenous injection at the tail.

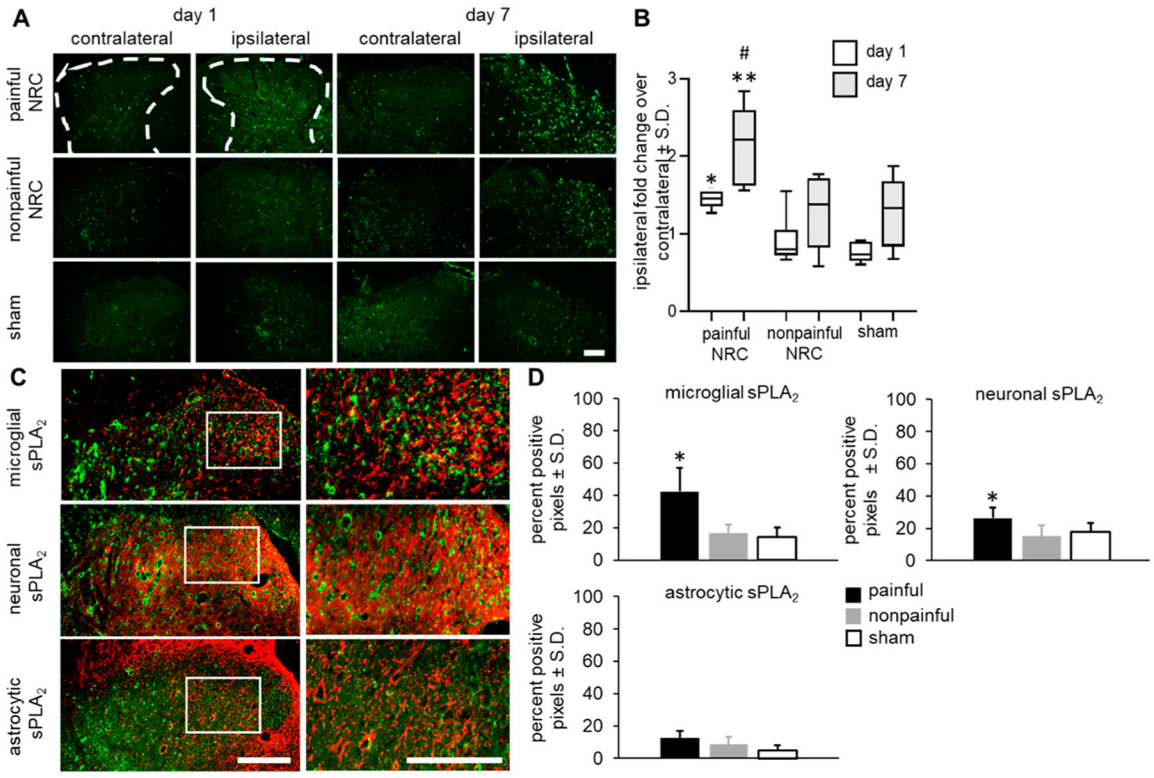

Figure 2.

Spinal $sPLA_2$ expression increases after a painful compression. (A) Representative images of the bilateral spinal dorsal horns show increased $sPLA_2$ immunoreactivity only in the ipsilateral spinal cord in all groups at day 7 compared to expression at day 1, with greatest expression in the painful group at each day. The scale bar is 200 μm and applies to all panels. (B) Quantification of $sPLA_2$ expression shows the painful group is significantly greater than expression after both a nonpainful compression and sham surgery on both days 1 (*$p < 0.048$) and 7 (**$p < 0.009$). Expression in the painful group at day 7 is significantly higher than levels at day 1 ($^{\#}p < 0.043$). (C) Representative images show the greatest extent of $sPLA_2$ immunoreactivity with microglia. The scale bar is 100 μm for lower magnification images and 50 μm for higher magnification panels (white box). (D) At day 1 after painful injury, both microglial ($p < 0.006$) and neuronal ($p < 0.038$) $sPLA_2$ expression is significantly higher than the nonpainful and sham groups. There were no significant differences in astrocytic $sPLA_2$ expression between groups.

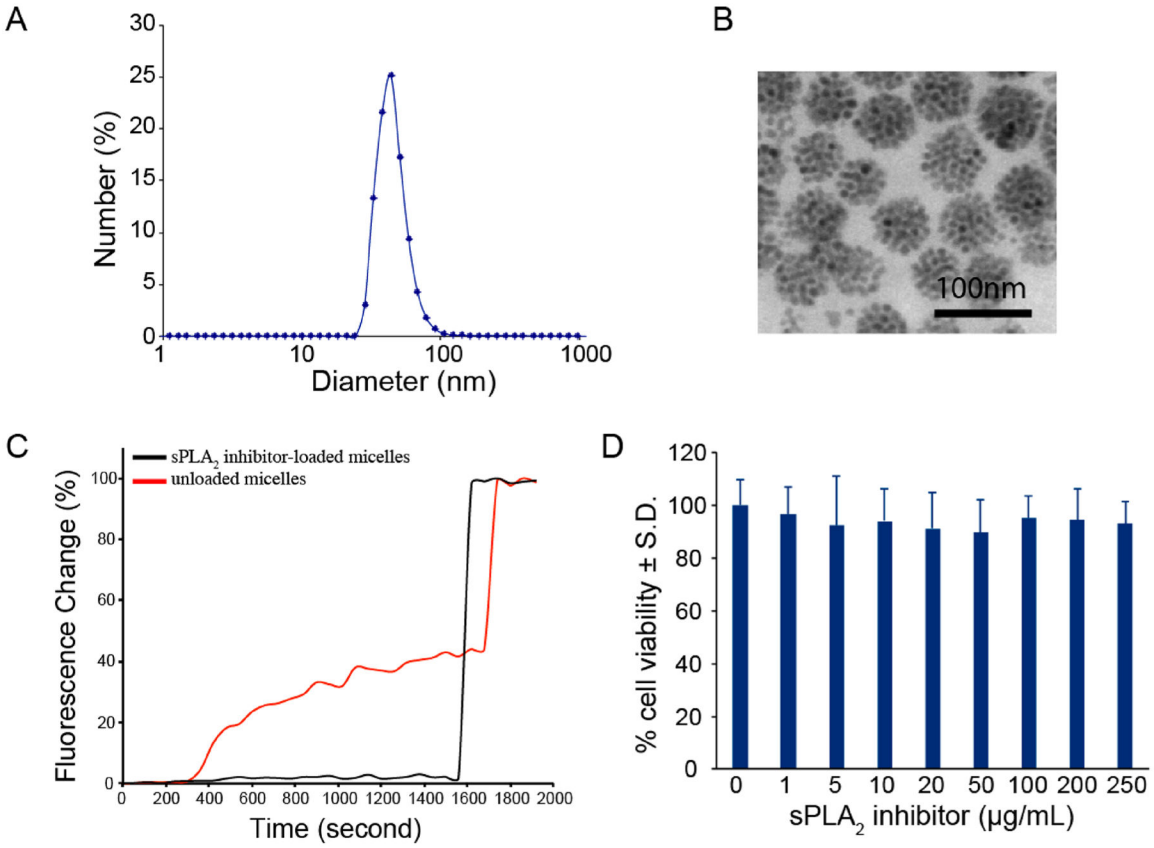

Figure 3.

Characterization of $sPLA_2$ inhibitor and SPIO-loaded phospholipid micelles. (A) Number-weighted size distribution of $sPLA_2$ inhibitor-loaded micelles by dynamic light scattering (DLS). The average hydrodynamic diameter is 60 nm. (B) Transmission electron microscopy (TEM) image of $sPLA_2$ inhibitor-loaded micelles. The electron micrograph shows tightly packed SPIONs within the hydrophobic core (scale bar: 100 nm). (C) *In vitro* response of $sPLA_2$ inhibitor-loaded micelles. $sPLA_2$ inhibitor-loaded micelles significantly inhibit PLA_2 activity. (D) Incubation of the $sPLA_2$ inhibitor-loaded micelles with rat dorsal root ganglion cells does not decrease cell viability from control (0 μg/mL) for any loaded concentration of $sPLA_2$ inhibitor.

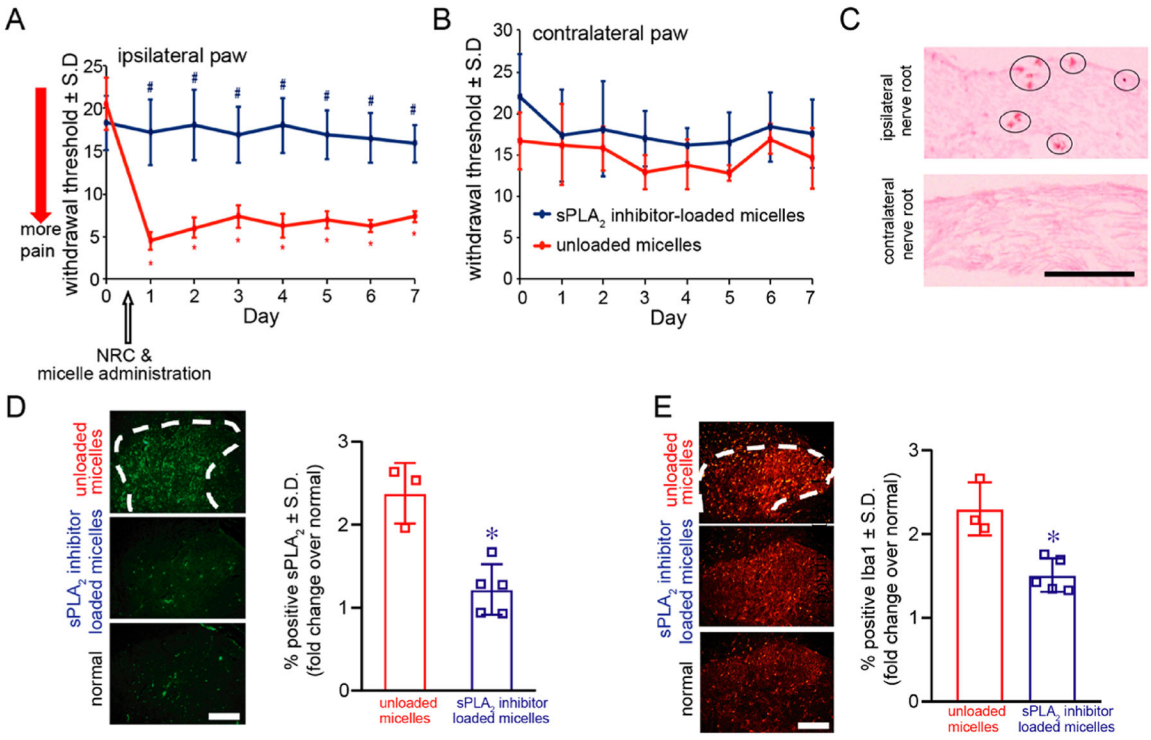

Figure 4.

Local administration of $sPLA_2$ inhibitor-loaded micelles immediately after a painful neuropathic nerve root compression injury prevents the development of pain and reduces the spinal $sPLA_2$ and Iba1 expression. (A) Ipsilateral paw withdrawal thresholds following treatment with $sPLA_2$ inhibitor-loaded micelles are significantly higher ($^{\#}p < 0.016$) than thresholds following treatments with micelles alone and are maintained at preinjury (day 0) levels. Administration of control micelles does not prevent pain, with withdrawal thresholds significantly lower than preinjury levels, lasting for 7 days ($^{*}p < 0.0001$). (B) The withdrawal threshold in the contralateral paw is not different between groups on any day tested. (C) $sPLA_2$-inhibitor- and SPIO-loaded micelles are found to localize at day 7 to the injured nerve root after local administration at the time of injury (day 0). Iron is detected (circles) only in the ipsilateral C7 dorsal nerve root after a nerve root compression. There is no evidence of iron in the contralateral C7 nerve root. The scale bar is 100 μm and applies to all panels. (D) $sPLA_2$ expression is significantly decreased ($^{*}p < 0.0001$) for treatment with $sPLA_2$ inhibitor-loaded micelles compared to levels treated with control unloaded micelles and is comparable to normal levels. (E) Spinal Iba1 expression is also decreased ($^{*}p = 0.0002$) at day 7 after treatment with $sPLA_2$ inhibitor-loaded micelles compared to treatment with unloaded micelles alone. The scale bars are 100 μm in all panels.

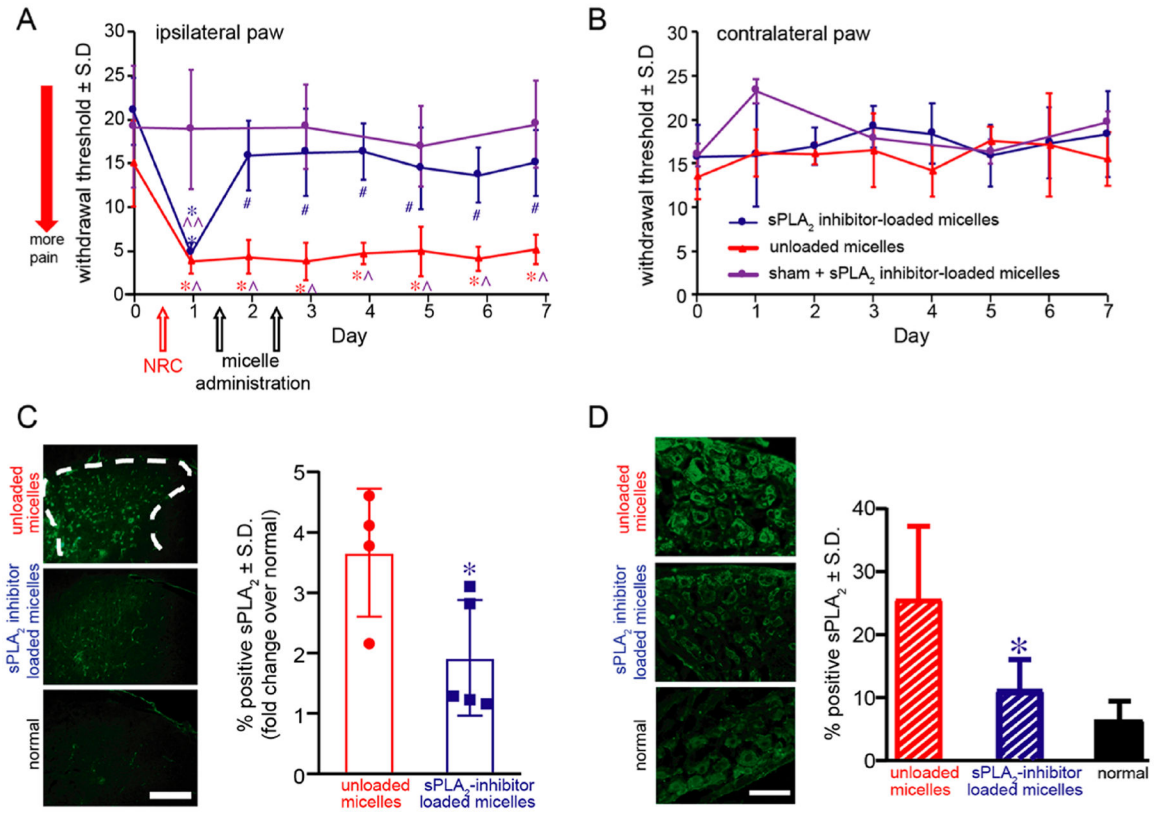

Figure 5.

Repeated intravenous (i.v.) administration of $sPLA_2$ inhibitor-loaded micelles on days 1 and 2 after painful nerve root compression (NRC) abolishes pain until day 7 and decreases $sPLA_2$ expression in the spinal cord and dorsal root ganglia (DRG) at day 7. (A) A painful NRC neuropathic injury significantly reduces withdrawal thresholds in the ipsilateral forepaw from preinjury (day 0) by day 1 ($^{\wedge}p = 0.0053$) and compared to thresholds after a sham surgery ($^{*}p = 0.001$). Withdrawal thresholds remain significantly decreased from sham withdrawal thresholds ($^{\wedge}p < 0.002$) after repeated administration on days 1 and 2 of control unloaded micelles (without PLA_2 inhibitor) for up to 7 days. Similarly, prior to treatment with $sPLA_2$ inhibitor-loaded micelles, thresholds on day 1 are significantly lower than those of the preinjury response on day 0 ($^{\#}p = 0.0001$) and sham responses on day 1 ($^{**}p = 0.0004$). Within 1 day of the i.v. micellar inhibitor treatment on day 1, withdrawal thresholds are significantly increased back to preinjury and sham response levels by day 2 and remain significantly elevated ($^{*}p < 0.0024$) through day 7. (B) There are no differences in the contralateral withdrawal thresholds for any of the groups. (C) Spinal $sPLA_2$ expression is significantly decreased ($^{*}p = 0.038$) in the superficial dorsal horn after treatment of micelles with inhibitor compared to treatment with unloaded micelles alone. Representative images are shown with a scale bar (100 μm) that applies to all panels. (D) Peripheral $sPLA_2$ expression in the DRG is also significantly ($^{*}p = 0.002$) reduced after treatment with $sPLA_2$ inhibitor-loaded micelles and is comparable to normal levels.